

Incidental emergency vascular pathologies on [18F] FDG-PET/CT and their metabolic patterns: a case series

Abstract

Purpose: We aim to review the image patterns of incidental vascular diseases on 2-deoxy-2-[18F]fluoro-D-glucose ([18F]FDG) Positron Emission Tomography/Computed Tomography (PET/CT).

Material and methods: A retrospective review of [18F]FDG PET/CT examinations at the Nuclear Medicine Unit of Queen Elizabeth Hospital Hong Kong was performed, focusing on detections of emergency vascular pathologies, in correlation with the clinical history and other radiologic modalities and we analyzed the unique metabolic patterns observed in these cases.

Results: Our analysis demonstrated that [18F]FDG PET/CT scans exhibited distinctive metabolic patterns associated with emergency vascular pathologies, including intracranial hemorrhage, portal venous thrombosis and deep venous thrombosis. These patterns provided valuable insights not evident in plain CT of PET/CT, enhancing the detection and characterization of the critical conditions.

Conclusion: Our study highlights the significance of recognizing the metabolic patterns associated with unexpected vascular pathologies, thereby enhancing diagnostic capabilities and patient outcomes.

Keywords: FDG, PET/CT, metabolic imaging, vascular disease, vascular emergency

Volume 11 Issue 5 - 2024

Wai Ip LI, Koon Kiu NG, Boom Ting KUNG

Nuclear Medicine Unit, Department of Diagnostic and Interventional Radiology, Queen Elizabeth Hospital, Hong Kong

Correspondence: Wai Ip Li, Nuclear Medicine Unit, Lower Ground Floor, Block K, Queen Elizabeth Hospital, 30 Gascoigne Road, Yau Ma Tei, Hong Kong, Tel +852-35068888, Email lwil89@ha.org.hk

Received: August 23, 2024 | **Published:** September 06, 2024

Introduction

2-deoxy-2-[18F]fluoro-D-glucose ([18F]FDG) Positron Emission Tomography/Computed Tomography (PET/CT) has revolutionized oncology by providing comprehensive metabolic and whole-body evaluations, enabling the identification of unexpected findings, including clinically significant vascular pathologies that occur at a higher prevalence in oncologic patients. However, plain CT in PET/CT is not sufficiently sensitive for detecting vascular pathologies, while the metabolic information obtained from PET plays a vital role in the assessment of such conditions. In this retrospective review of [18F]FDG PET/CT scans done in our local nuclear medicine centre, we aim to review and demonstrate the specific metabolic patterns of different incidental vascular pathologies on the images.

Material and methods

Patient selection

We retrospectively reviewed [18F]FDG PET/CT examinations performed at the Nuclear Medicine Unit of Queen Elizabeth Hospital Hong Kong in the past five years. The images with incidental vascular pathologies on [18F]FDG PET/CT reports were retrieved for further analysis.

Image protocol

For our patient preparation for the [18F]FDG PET/CT, we followed the international standard.^{1,2} Patients fasted for at least 4 hours before tracer injection. Plasma glucose levels were checked to ensure < 11mmol/L upon arrival at our PET centre. Intravenous administration of [18F]FDG of 10 mCi (370 MBq) was given, followed by PET/CT

acquisition after an uptake interval of 60 minutes. [18F]FDG PET/CT scans were performed using a PET/CT system, Discovery 710 (GE Healthcare, Milwaukee, WI, USA). PET images were acquired using the 3D acquisition mode with a duration of 2 minutes per bed position covering from vertex to mid-thigh or to the toes if indicated. Ordered subset expectation maximization (OSEM) with time-of-flight and point spread function modeling was applied, utilizing 4 iterations and 18 subsets, with a 5.5mm cutoff filter. Slice thickness was set at 3.27mm and a matrix size of 256 x 256. CT was acquired using the helical mode with a voltage of 120 kVp and a current ranging from 80 to 400 mA, modulated with a noise index of 15. Rotation speed was set at 0.5 sec/rot with a pitch of 0.984. Slice thickness and increment were set at 3.75 mm and 3.27 mm, respectively. Matrix size was set at 512 x 512.

Image analysis

Nuclear medicine physicians with at least five years of experience in molecular imaging evaluated the [18F]FDG PET/CT images using the Volume Viewer (Advanced Workstation version 12.3, Ext 8; GE Healthcare, Milwaukee, WI, USA), focusing on detections of emergency vascular pathologies, in correlation with the clinical history and other radiologic modalities, and analyzing the unique metabolic patterns observed in these cases.

Ethical standards

This study was performed in line with the principles of the Declaration of Helsinki. Approval was granted by the Central Institutional Review Board of the Hospital Authority, Hong Kong (reference number: CIRB-2024-274-4). Informed consent was waived due to the retrospective nature of the study.

Results

Case 1

An 83-year-old woman, previously diagnosed with diffuse large B-cell lymphoma six years ago, achieved complete metabolic remission post-chemotherapy. She presented with persistent low-grade fever, leading to the discovery of a recurrent diffuse large B-cell lymphoma. The initial baseline [18F]FDG PET/CT scan revealed hypermetabolic mediastinal nodal masses. Following four cycles of chemotherapy, a subsequent end-of-treatment scan displayed a new hypermetabolic abdominal node, indicative of disease progression compared to the baseline scan (Figure 1). Additionally, an incidental finding of left crossed cerebellar diaschisis was noted on the maximum intensity projection (MIP) and transaxial images, alongside a hyperdense lesion in the right internal capsule suggestive of an acute hematoma (Figure 2 and 3). Unfortunately, the patient's condition deteriorated, and she passed away one month later due to multi-organ failure.

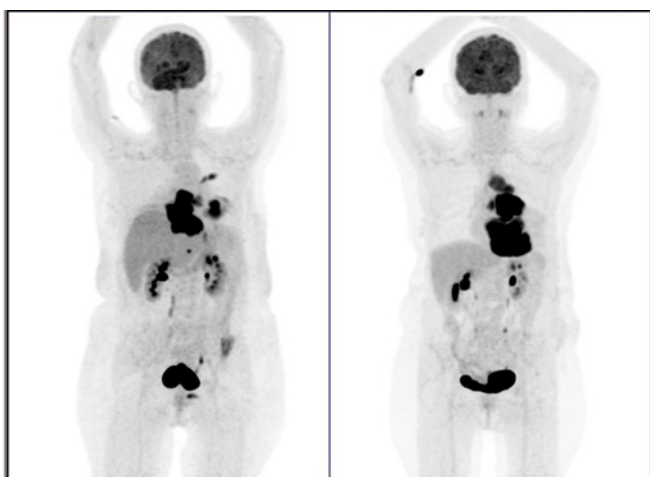


Figure 1 Maximal intensity projection (MIP) images from [18F]FDG PET/CT scans illustrating the end-of-treatment (left) and baseline (right) scans of an 83-year-old woman with recurrent lymphoma undergoing chemotherapy. The end-of-treatment scan, conducted after four cycles of chemotherapy for recurrent lymphoma, revealed a new hypermetabolic upper abdominal node and persistent supradiaphragmatic nodal masses, indicative of disease progression. Additionally, an incidental finding of new left crossed cerebellar diaschisis was observed, reflecting new brain pathology.

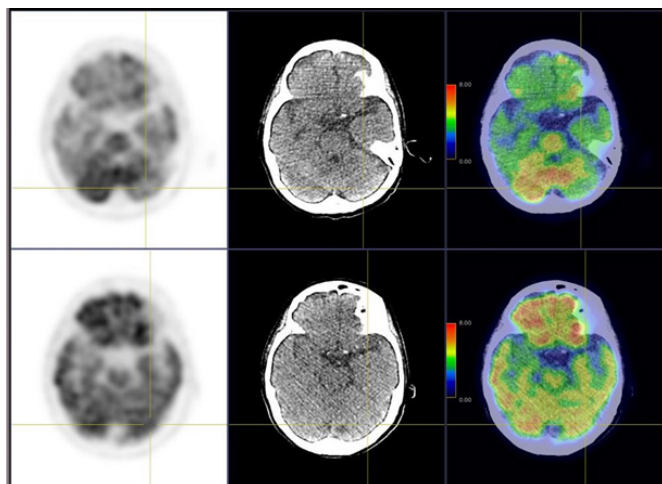


Figure 2 Comparison of transaxial PET, CT, and fusion images from the end-of-treatment scan (upper row) and baseline scan (bottom row). The images depict reduced left cerebellar activity in the new scan.

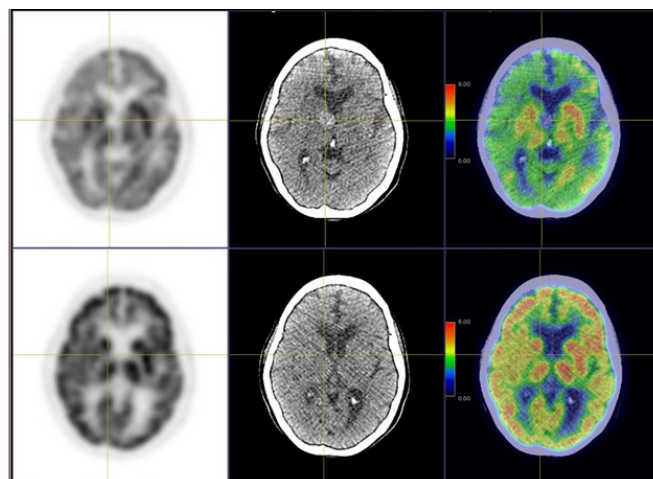


Figure 3 Comparison of transaxial PET, CT, and fusion images from the end-of-treatment scan (upper row) and baseline scan (bottom row). A new photopenic hyperdense lesion at the right internal capsule, consistent with a hematoma, was observed. The reduced activity in the right cerebral region, along with decreased left cerebellar activity, indicated left crossed cerebellar diaschisis.

Case 2

A 75-year-old man presented with blood-stained sputum and diminished appetite. A contrast CT of the thorax revealed a mass in the right upper lobe of the lung with enlarged mediastinal lymph nodes, without signs of organ metastases. A CT-guided biopsy confirmed poorly differentiated non-small cell carcinoma. A subsequent staging [18F]FDG PET/CT, conducted one month later, exhibited a hypermetabolic large mass in the right upper lobe of the lung, along with mediastinal lymph nodes and multiple bone lesions (Figure 4). Notably, there was marked patchy activity in the left liver lobe with new slight hypodense changes and enlargement, raising suspicion of an acute pathology. Further assessment through contrast imaging was recommended. A follow-up contrast CT, performed nine days later, revealed a filling defect in the left portal vein (Figure 5). The patient's health declined, and he passed away three days after admission due to metabolic acidosis and respiratory failure.



Figure 4 MIP image from the staging [18F]FDG PET/CT scan of a 75-year-old man newly diagnosed with lung cancer. The scan revealed a hypermetabolic mass in the right upper lobe of the lung, thoracic nodal metastases, and multiple bone metastases. Additionally, marked patchy activity in the left liver lobe with enlargement was noted.

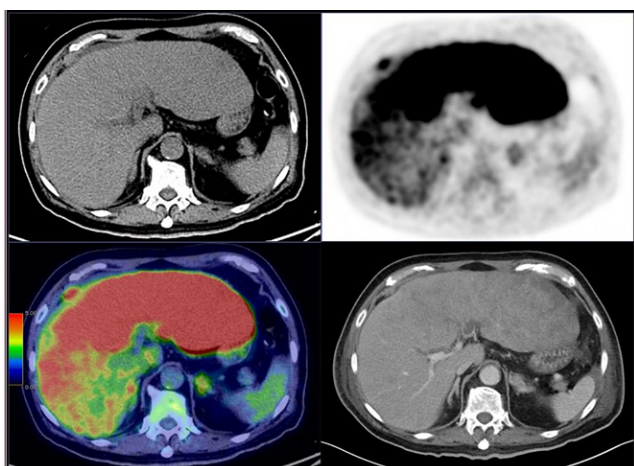


Figure 5 Transaxial CT, PET and fusion images from the [18F]FDG PET/CT scan and a contrast CT performed nine days later. An incidental marked patchy activity in the left liver lobe on PET, along with slight hypodense changes and enlargement on plain CT, was observed. The subsequent contrast CT confirmed a filling defect in the left portal vein, indicative of portal venous thrombosis.

Case 3

A 40-year-old man presented with a prolonged fever of unknown origin, prompting a [18F]FDG PET/CT scan to investigate potential sources of infection or inflammation. The imaging revealed

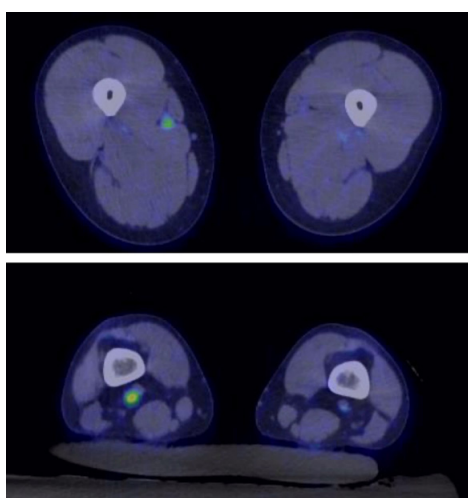


Figure 7 Fusion [18F]FDG PET/CT images displaying asymmetrical activity along the right femoral vein and right popliteal vein in the lower extremities.

Discussion

The utilization of [18F]FDG PET/CT has become increasingly prevalent in contemporary medical imaging practices, particularly in the diagnosis and management of oncological disorders. However, it is crucial to recognize that patients undergoing such imaging procedures may be predisposed to heightened risks of vascular complications, including thromboembolic events and hemorrhage. These vulnerabilities are often attributed to both the complexities associated with malignancies and the therapeutic interventions employed in cancer treatment.³

hypermetabolic consolidation in the left lower lung, alongside incidental asymmetrical activity in the right femoral vein and right popliteal vein (Figure 6 and 7). Doppler ultrasonography images of the right lower limb showing non-compressibility in the right femoral and right popliteal veins, along with the presence of echogenic thrombi, confirming a diagnosis of deep venous thrombosis (Figure 8). Patient remains well after anti-coagulation therapy.

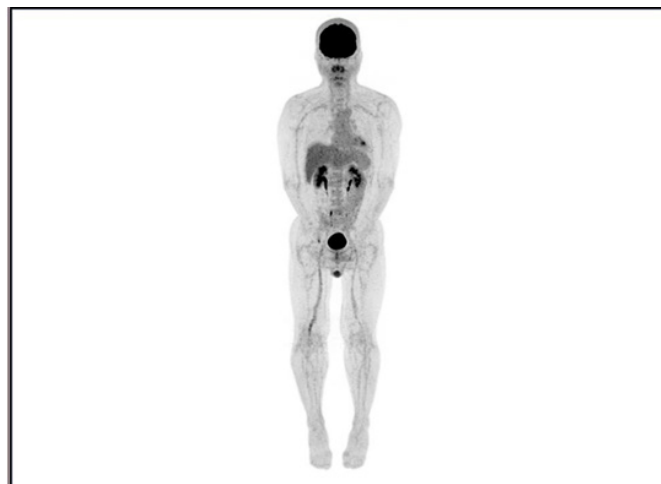


Figure 6 MIP image from the staging [18F]FDG PET/CT scan of a 40-year-old man with fever of unknown origin. The scan exhibited hypermetabolic consolidation in the left lower lung lobe, along with asymmetrical activity in the right femoral vein and right popliteal vein.

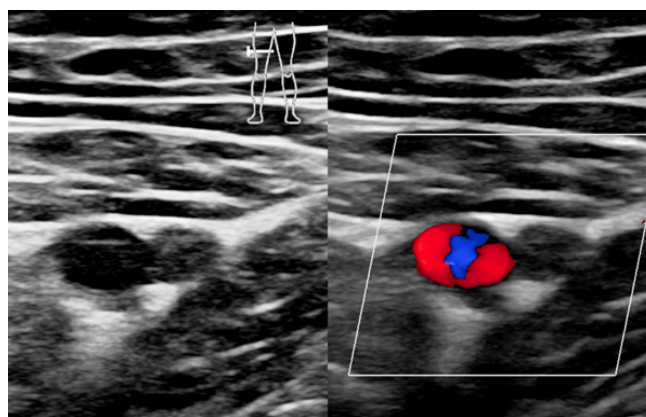


Figure 8 Doppler ultrasonography images of the right lower limb showing non-compressibility in the right femoral and right popliteal veins, along with the presence of echogenic thrombi, confirming a diagnosis of deep venous thrombosis.

[18F]FDG PET/CT, renowned for its comprehensive evaluation spanning from the cranial region down to the lower extremities, occasionally unveils unforeseen yet clinically significant incidental findings, some of which pertain to vascular pathologies. In a series of cases we examined, three instances of vascular ailments with distinct metabolic signatures were elucidated in the imagery: hemorrhagic stroke, portal venous thrombosis, and deep venous thrombosis.

One notable phenomenon observed in our review of cases is the crossed cerebellar diaschisis, a condition typified by radiological or scintigraphic manifestations of diminished perfusion and metabolic

activity in the cerebellar hemisphere contralateral to cerebral lesions. Etiological factors encompass hemorrhagic or ischemic strokes, primary and secondary brain neoplasms, as well as functional brain disorders like epilepsy or encephalitis.⁴⁻⁶ In our case, an unanticipated hematoma in the right internal capsule underscored the necessity for vigilant monitoring and further diagnostic exploration to avert potential deterioration and rule out tumor-related bleeding. Given the limitations of conventional low dose plain CT of PET/CT in detections of brain pathologies, the metabolic insights provided by PET play a pivotal role in detecting such diseases.

The distinctive metabolic profile associated with portal venous thrombosis has been documented in previous investigations, with [18F]FDG PET/CT serving as a valuable tool in detection of portal venous thrombosis, which contributes to significant morbidity and mortality, and discerning between bland thrombi and tumor emboli.⁷⁻⁹ This differentiation is instrumental in guiding tailored treatment strategies. In our case, the absence of metabolic uptake at the portal venous thrombus indicated its benign nature, a diagnosis further corroborated by contrast-enhanced CT imaging. The high diffuse metabolic activity within hepatic tissues of thromboembolic regions may signal secondary inflammation due to ischemia, a vital scintigraphic sign that likely serves as the sole clue in a non-contrast PET/CT, warranting confirmation with a contrast study.

Similarly, the metabolic characteristics of deep venous thrombosis have been elucidated in prior studies, with [18F]FDG PET/CT offering insights into distinguishing acute from chronic clot formations based on uptake intensity.¹⁰ Nonetheless, it is imperative to underscore that while PET/CT imaging provides valuable metabolic data, the diagnosis of deep venous thrombosis still necessitates the integration of physical examination and doppler ultrasonography. This integrated approach to the prompt diagnosis is essential for guiding appropriate treatment strategies and preventing serious complications such as pulmonary embolism. Imaging specialists interpreting such findings should advocate for additional investigations to ensure a thorough and patient-centered care plan.

Conclusion

Our study highlights the significance of recognizing the metabolic patterns associated with unexpected vascular pathologies, thereby enhancing diagnostic capabilities and patient outcomes. The integration of metabolic information obtained from [18F]FDG PET/CT is essential for recognizing and managing emergency vascular pathologies. By leveraging this imaging modality in daily practice, nuclear medicine physicians and radiologists can improve patient care by facilitating early intervention and potentially reducing associated mortality rates.

Conflict of Interest

None to declare.

Acknowledgments

None

References

1. Boellaard R, Delgado-Bolton R, Oyen WJ, et al. FDG PET/CT: EANM procedure guidelines for tumour imaging: version 2.0. *Eur J Nucl Med Mol Imaging*. 2015;42(2):328–354.
2. Jamar F, Buscombe J, Chiti A, et al. EANM/SNMMI guideline for 18F-FDG use in inflammation and infection. *J Nucl Med*. 2013;54(4):647–658.
3. Akhter N. Vascular disease in cancer: Current and emerging concepts. *Am Heart J Plus*. 2022;17:100143.
4. Han S, Wang X, Xu K, Hu C. Crossed cerebellar diaschisis: three case reports imaging using a tri-modality PET/CT-MR System. *Medicine (Baltimore)*. 2016;95(2):e2526.
5. Mewasingh LD, Christiaens F, Aeby A, et al. Crossed cerebellar diaschisis secondary to refractory frontal seizures in childhood. *Seizure*. 2002;11(8):489–493.
6. Thajeb P, Shih BF, Wu MC. Crossed cerebellar diaschisis in herpes simplex encephalitis. *Eur J Radiol*. 2001;38(1):55–58.
7. Surasi DS, O'Malley JP, Bhambhani P. 18F-FDG PET/CT findings in portal vein thrombosis and liver metastases. *J Nucl Med Technol*. 2015;43(3):229–230.
8. Erhamamci S, Reyhan M, Nursal GN, et al. Incidental diagnosis of tumor thrombosis on FDG PET/CT imaging. *Rev Esp Med Nucl Imagen Mol*. 2015;34(5):287–294.
9. Hu S, Zhang J, Cheng C, et al. The role of 18F-FDG PET/CT in differentiating malignant from benign portal vein thrombosis. *Abdom Imaging*. 2014;39(6):1221–1227.
10. Rondina MT, Lam UT, Pendleton RC, et al. (18)F-FDG PET in the evaluation of acuity of deep vein thrombosis. *Clin Nucl Med*. 2012;37(12):1139–1145.